International Journal of Modern Manufacturing Technologies
ISSN 2067–3604, Special Issue, Vol. XIII, No. 3 / 2021
https://doi.org/10.54684/ijmmt.2021.13.3.164

NUMERICAL SIMULATION OF TRI-LAYERED MATERIALS UNDER CONTACT LOAD

Sergiu Spinu[1,2]

[1] Department of Mechanics and Technologies, Stefan cel Mare University of Suceava,
13th University Street, 720229, Romania
[2] Integrated Center for Research, Development and Innovation in Advanced Materials, Nanotechnologies and Distributed Systems for Fabrication and Control (MANSiD), Stefan cel Mare University, Suceava, Romania

Corresponding author: Sergiu Spinu, sergiu.spinu@fim.usv.ro

Abstract: Various biomedical components, such as dental crowns and hip prostheses, data processing devices, and other numerous mechanical components that transmit load through a mechanical contact, may benefit from a tri-layer design. The coating may be optimized for wear protection and corrosion prevention, whereas the intermediate layer provides increased adhesion between the outer layer and the substrate, and confines the crack propagation. The solution to the contact problem involving tri-layered materials can be pursued numerically with the finite element or the boundary element methods, but semi-analytical techniques benefitting from the efficiency of the fast Fourier transform (FFT) technique have also been successfully applied. At the heart of the FFT-assisted approach lie the frequency response functions (FRFs), which are analytical solutions for fundamental problems of elasticity such as the Boussinesq and Cerruti problems, but expressed in the frequency domain. Considering recent efforts and results in application of FFT to convolution calculations in contact problems, the displacement arising in a tri-layer configuration is computed in the frequency domain, and the contact problem is subsequently solved in the space domain using a state-of-the-art algorithm based on the conjugate gradient method. The method relies on the FRFs derived in the literature for tri-layered materials, and the efficiency and accuracy of computations in the frequency domain is assured by using the Discrete Convolution Fast Fourier Technique (DCFFT) with influence coefficients derived from the FRFs. The computer program reproduces well-known results for bi-layered materials. Numerical simulations are performed for various configurations in which the elastic properties of the layers, as well as the frictional coefficient, are varied. By using the newly advanced simulation technique, design recommendations may be advanced for the optimal configuration of tri-layered materials under contact load.

Key words: elastic contact, multilayer materials, fast Fourier transform, frequency response functions.

1. INTRODUCTION

Various mechanical components used in biomedical or data-processing devices consist in an outer layer on a substrate, and having one intermediate layer. Such tri-layer materials are often encountered in dental crowns and hip prostheses, as well as in hard disks, gears or bearings, and can be modelled by an elastic half-space, i.e., the substrate, and two perfectly bonded coatings of finite thickness. The role of the outer layer is to improve the corrosion prevention and wear protection of the component, whereas the intermediate layer provides better adhesion between the coating and the substrate.

The study of the configuration that optimises the performance of the layered system to better accommodate contact load is a subject of interest [1, 2] considering the cracking and damage modes that affect the contact fatigue life. With analytical solutions lacking even for homogeneous materials under contact load, various specialised numerical methods were developed in computational contact mechanics, seeking numerical solutions for the contact area, deformation and stresses arising in the contacting bodies: (a) the finite element method [3-8], (b) the boundary element method [9], (c) the equivalent inclusion method [10-12], and (d) the semi-analytical method (SAM) [13-22]. The latter is particularly efficient when coupled with Fourier transform algorithms that provide means for rapid calculation of convolution products, by converting the tedious integration operation from the problem space domain, into element-wise multiplication in an associated frequency domain. Considering that the mathematical relation between a surface excitation and a stress response in the contacting body is generally in form of a convolution, great computational efficiency is attained, which further supports iterative processes for finding the remaining model unknowns.

The treatment of the contact problem of layered materials using SAM relies on the description of the body response to a unit force (a half-space fundamental solution to an elementary problem), which is furthermore integrated numerically to obtain

the response to a surface arbitrary load. The fundamental solution for layered materials was obtained in closed-form in the frequency domain only, and is referred to as the frequency response function (FRF). Resolution of the contact problem based on the FRFs, as well as the calculation of the FRFs themselves, are topics of intense research efforts [15-22] in the last two decades.

This paper continues and extends previous works [21,22] concerning the contact of bi-layered materials, to the case of tri-layered configurations. The FRFs existing in the literature [17,20] are converted into influence coefficients that can be used in a Discrete Convolution Fast Fourier Transform (DCFFT) algorithm [23] to efficiently perform the convolution calculations. The influence of the frictional coefficient and of the elastic properties mismatch is then studied by numerical simulation.

2. CONTACT MODEL OVERVIEW

The discrete contact model employed in this paper is similar to the one described in [24], and features a contact zone discretization performed with a rectangular uniform grid and piece-wise constant distributions of problem parameters. Whereas the finite element method may benefit from adaptive meshes that concentrate nodes in the regions with high gradients, SAM is restricted to a constant grid step (that can however be different on any of the two tangential directions) to limit the number of different influence coefficients that need to be computed for the DCFFT.

The input of the contact problem consists in: (a) the elastic properties and the geometrical configuration of the contacting materials, (b) the normal load transmitted through the contact, and (c) the frictional coefficient, assumed uniform on the contact area. A few additional assumptions, classic to contact mechanics, are further required to achieve a solvable mathematical model: (a) the contacting bodies are approximated with elastic half-spaces, which is reasonable for concentrated contacts, (b) the contact interface is without adhesion, and (c) there is no body interpenetration in the frame of elastic theory of elasticity. The first assumption authorizes the use of the fundamental solutions derived for the elastic half-space in computation of the body response, whereas the other two allow for the solution of the contact problem via quadratic optimization [25].

A schematic of the contact process is depicted in Figure 1. A concentrated point contact is typically reduced based on the equivalent punch theory to a spherical rigid indenter pressed against an elastic half-space. The spherical indenter comprises the contact geometry data, whereas the half-space encompasses the contact compliance (i.e., the contribution of the elastic properties of the contacting materials). The elastic properties are denoted as follows: ν_i and $E_i, i=1,2,3$, are the Poisson's ratios and the Young moduli of the elastic layers, with $i=1$ for the coating, $i=2$ for the intermediate layer, and $i=3$ for the substrate. It should be noted that although the schematic in figure 1 is in a radial plane, the developed contact model is actually three dimensional.

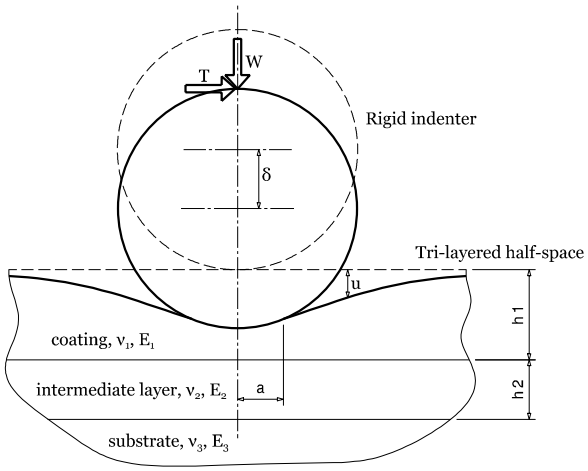

Fig. 1. Schematic of the contact process

Under the action of the normal force W, the contacting bodies approach each other with a quantity δ known as the rigid-body approach, and a contact area of radius a is established, on which a pressure distribution counterbalances the applied force. Subsequently, a tangential force T large enough as to induce gross slip, is applied.

The expected model output consists in: (a) the shape and size of the contact area, (b) the distribution of contact tractions (pressure and shear), and (c) the stress field developed in the contacting bodies in response to the latter contact tractions. By adopting the assumption of a contact in full slip, the number of unknowns is decreased and the model complexity is greatly reduced, as the contact subproblems in the normal and in the tangential are decoupled. Practically, the contact solution can be achieved in the following steps:

1. Solve the frictionless contact problem assuming vanishing shear tractions. Obtain the contact area and the pressure distribution.
2. Derive the shear tractions from the Coulomb friction law.
3. Compute the subsurface stresses induced by either the normal or the shear contact tractions.
4. Superimpose the stress distributions to obtain the contact stress state.

The above steps can be executed once a method for calculation of displacement induced in a layered material by an arbitrary, yet known, distribution of

pressure, is established. By adopting the SAM related formulation, displacement is obtained by integration of a fundamental solution for the elastic half-space (i.e., the Boussinesq solution for a normal point force acting on the boundary of a homogeneous half-space) over the contact area. A particular feature of the problem model is that not only the pressure distribution, but also the contact area, are unknown and must be derived simultaneously in an iterative process, based on the conjugate gradient method [24]. Such solution strategy requires an integration technique that is both robust and computationally efficient. These requirements are met by the Fourier transform algorithm described in the following section.

3. DISPLACEMENT COMPUTATION

Unlike the case of a homogeneous half-space, for which the Boussinesq solution was derived in closed-form, stresses and displacements induced in a layered half-space by a point force are not available analytically at the time of this work. The closed-form solution to the latter fundamental problem exists only in the frequency domain, and is known as the FRF. The main challenge when using this solution is to contain the error that appears when discretization is employed in the frequency domain. The transfer to and from the space domain to the frequency domain is achieved via the fast Fourier transform (FFT), which is a collection of very efficient algorithms for calculation of the discrete Fourier transform. The main idea of the FFT-based algorithms applied in contact mechanics to compute convolutions products, is to substitute the integration in the space domain, which is very computationally intensive, by an element-wise product in the frequency domain, as postulated by the convolution theorem. The computational advantage is significant: a reduction in the order of operations from $O(N^2)$ to $O(N\log N)$ for the convolution of two series, each having N terms. An additional complication arises as the concentrated contact problem is essentially non-periodic, while FFT applied to discrete series tacitly assumes periodicity. Practically, the calculated displacement is not only due to the initial pressure distribution, but comprises contributions from an infinite number of pressure periods identical to required one. Special algorithm treatments can entirely eliminate this periodicity error [15,23] without affecting the computational efficiency, as described below.

From the various types of convolution theorems [26], the appropriate one for the non-periodic contact problem is the so-called cyclic (circular) convolution. Although the model reported in this paper is three dimensional, thus involving a 2D convolution computation, in this section the model equations are presented in one dimension only for brevity. Let $K(i)$ and $p(i)$, $i=1\ldots N$, denote the discrete series of finite length N, whose convolution yields the elastic displacement: the former is the series of influence coefficients, and the latter the discrete pressure distribution. The discrete Fourier transforms of these series, calculated through FFT, are $\hat{K}(m)$ and $\hat{p}(m)$, with m the frequency variable and the hat ($\hat{x}$) symbol denoting spectral series. The element-wise product of the latter series:

$$\hat{u}(m)=\hat{K}(m)\cdot\hat{p}(m) \tag{1}$$

is in fact the circular convolution calculated in the span $1\ldots N$, and its expression in the space domain is:

$$u(j)=\sum_{i=1}^{N}K(j-i)\cdot p(i),\ 1\le j\le N, \tag{2}$$

or, to avoid the negative argument for the influence coefficients series:

$$u(j)=\sum_{i=1}^{N}K(j-i+N\cdot H(i-j))\cdot p(i),\ 1\le j\le N, \tag{3}$$

where $H(x)$ is the Heaviside unit step function that equals 1 for positive input and zero otherwise. The latter equation suggests the circular fashion of the influence coefficients series, and consequently the K series must be arranged in such a way for the circular convolution (1) to be properly performed. This is achieved by zero-padding and wrap-around order, as suggested in [23]. The required treatment to compute the circular convolution of the $K(i)$ and $p(i)$ series without any periodicity error is depicted in Figure 2. Although the series are for the $i=1\ldots N$ span, the influence coefficients must be computed in a $2N$ window centered in origin, and the terms for the negative side should be shifted after the positive ones, to fulfill the circular requirement. This arrangement is referred to as a wrap-around order. A vanishing value between the original and the shifted terms is introduced at $i=N+1$ (zero padding). On the other hand, the treatment for the pressure series only consists in zero-padding in the extended window $i=N+1\ldots 2N$.

Once the convolution series have been obtained in this arrangement, their discrete Fourier transforms are calculated through a FFT algorithm. The convolution result in a window twice the required one is obtained in the frequency domain by evaluation of relation (1).

Inverse FFT is then applied to the series $\hat{u}(m)$ for transfer back to the space domain. The resulting series of $2N$ terms in the space domain holds on the first N positions the required discrete displacement. Although the terms in the extended domain are eventually not used, they are required to assure the method consistency.

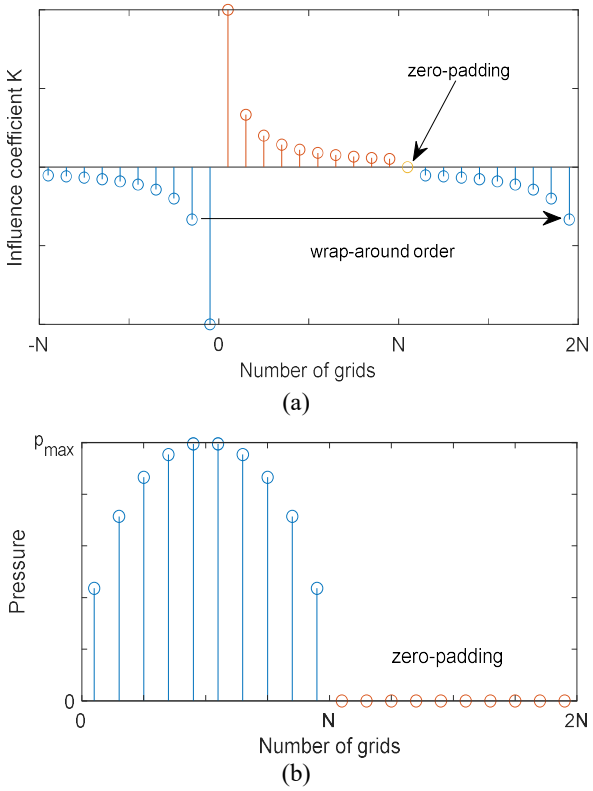

Fig. 2. The required treatment of series for circular convolution: a) zero-padding and wrap-around order for the influence coefficients series; b) zero-padding of the pressure series

Calculation of influence coefficients K in a $2N$ span for a homogeneous elastic half-space is performed based on the Boussinesq solution, as detailed in [24]. However, for the layered half-space, the closed-form solution of a counterpart Boussinesq problem (i.e., displacement induced by a point force acting on the half-space boundary) has only been calculated in the frequency domain. A special procedure for the derivation of the required influence coefficients was proposed in a previous work concerning bi-layered materials [21,11], and is also applied here for the tri-layered half-space. The FRFs for tri-layered materials are considerably more complex, and their calculation was performed based on the relations described in [17,20].

With the computational model described above, the stresses developing in a multi-layered system can be obtained by numerical simulation, with no additional error other than the discretization error, as described in the following section.

4. RESULTS AND DISCUSSIONS

The simulated contact process comprises a rigid spherical indenter pressed against a tri-layered half-space, as shown in Figure 1. The initial point of contact progresses into a circular contact area due to deformation of the elastic body under external load. Once the equilibrium contact area is established, the contact is subjected to a tangential force large enough to induces full-sliding. The stresses in the layered system are obtained by superposition of contributions from both pressure and shear tractions.

At this point, there exist no analytical solution for the indicated contact scenario. The only closed-form solution in contact mechanics theory, namely the Hertz contact, is used for normalization of results. The Hertz contact parameters are first calculated assuming the half-space is homogeneous and its elastic parameters coincide with those of the substrate, i.e., ν_3 and E_3. The resulting contact radius a_H, and the central pressure distribution p_H, normalize distances, and stresses, respectively. The magnitude of stresses in the layered body is described by the von Mises equivalent stress, which can be seen as a norm of the stress tensor, assessing the combined intensity of all the nine stress tensor components through a single scalar. This equivalent stress is also considered to best describe the propensity for plastic yield and therefore is often used for designing purposes.

A set of contact simulations was performed by varying the frictional coefficient and the Young moduli ratios of the three layers, while all others problem parameters were kept constant. Validation of the computer program is achieved by reducing the number of layers to two, and by comparison with literature results [13]. A good agreement was found with the model for bi-layered materials, either when $E_1 = E_2$, or when $E_2 = E_3$. The combined influence of the elasticity modulus ratios and of the frictional coefficient μ is suggested in Figures 3-5. In all cases, the thicknesses of the coating and of the intermediate layer were kept constant, $h_1 = h_2 = a_H/2$. Dimensionless coordinates were defined as ratio to the Hertz contact radius a_H, and dimensionless von Mises equivalent stress as ratio of the second stress tensor invariant J_2 to Hertz pressure p_H. The position of the maxim stress is indicated on each plot with an "X" symbol, and the magnitude of the dimensionless maximum is displayed above the plot.

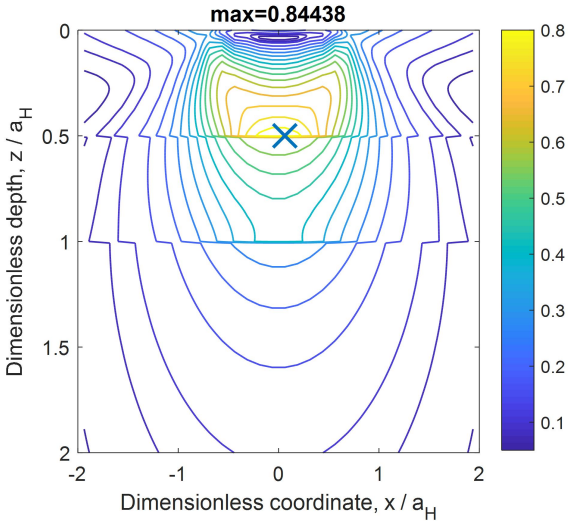

(a)

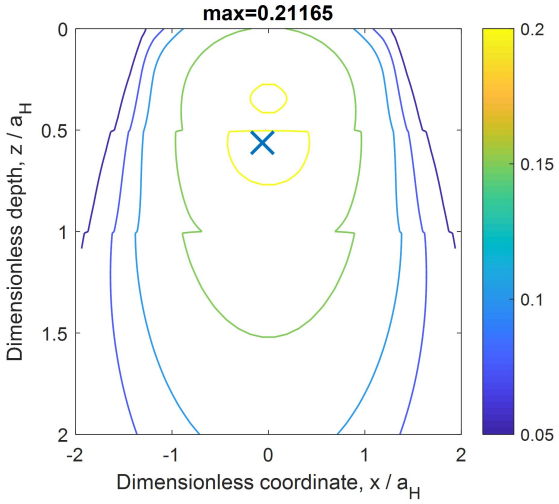

(b)

Fig. 3. Iso-contours of $\sqrt{J_2}/p_H$, $\mu = 0$:
a) $E_1 = 2E_2 = 4E_3$; b) $E_1 = 1/2\,E_2 = 1/4\,E_3$

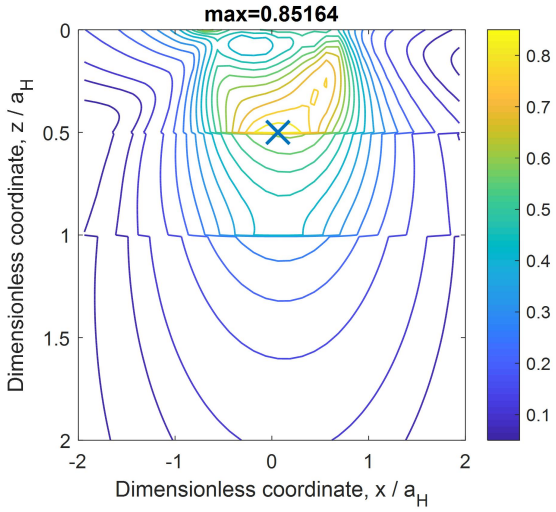

(a)

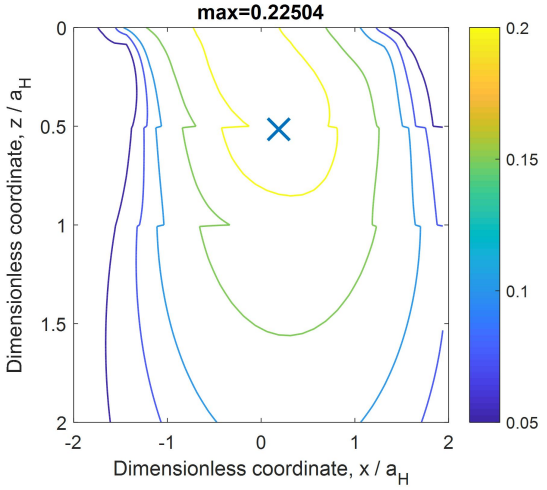

(b)

Fig. 4. Iso-contours of $\sqrt{J_2}/p_H$, $\mu = 0.25$:
a) $E_1 = 2E_2 = 4E_3$; b) $E_1 = 1/2\,E_2 = 1/4\,E_3$

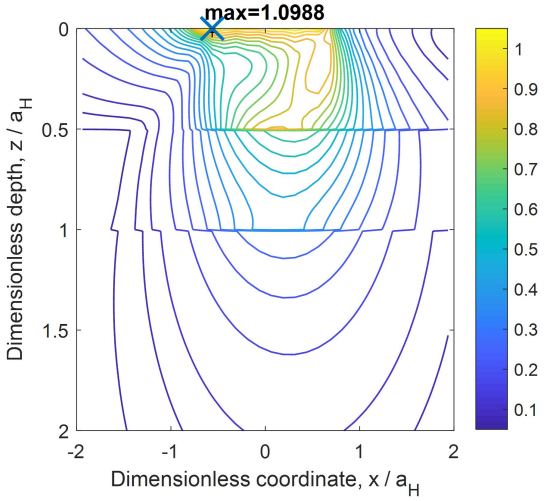

(a)

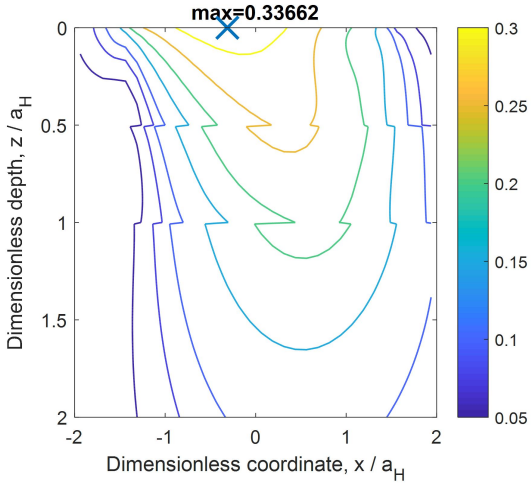

(b)

Fig. 5. Iso-contours of $\sqrt{J_2}/p_H$, $\mu = 0.5$:
a) $E_1 = 2E_2 = 4E_3$; b) $E_1 = 1/2\,E_2 = 1/4\,E_3$

Due to accumulation of rounding errors in calculation of discrete values of the FRFs, a relatively low-resolution grid of 32×32 points covering a rectangular domain of side lengths $4a_H$ was implemented. Further increase of the resolution resulted in numerical oscillations at the boundaries of the considered computational domain. Additional measures, including symbolic calculation of the influence coefficients, may be required, but this is left for a future study.

Due to this coarse grid, the maximums in Figure 3 appears to have an eccentric position, whereas the correct location is on the normal contact axis (at $x/a_H = 0$). In Figures 4 and 5, due to the influence of the shear tractions, the stress plots loose symmetry. The position of the maximum shifts toward the sliding direction for $\mu = 0.25$, and in the opposing direction for $\mu = 0.5$.

The depth of the maximum is also an important criterion for the optimum design of layered systems. Moving the maximum in a harder layer may provide advantages by delaying the plastic yield initiation. On the other hand, a localization at the interface between two layers was found in the literature to be problematic from the point of view of crack initiation. As shown in Figure 4, a frictional coefficient $\mu = 0.25$ proves particularly disadvantageous for the considered configurations.

The plots also show that an intense frictional regime moves the position of the maximum to the contact interface, as in the case of homogeneous materials. This is also suboptimal considering that at small depths there exist high stress gradients due to the inherent surface microtopography. Although these stresses are not covered in this study, as the considered model is smooth, there exist no conceptual difficulty in applying the current model to rough contacts, provided the computer program can handle finer meshes with limited computational resources.

5. CONCLUSIONS

The design of optimum configurations of tri-layered materials from the point of view of mechanical contact performance can only be achieved through numerical analysis, due to lack of analytical solutions in both contact mechanics and in the mathematical modelling of layered materials. This paper extends a technique simulation previously developed for bi-layered materials to the case of tri-layered bodies.

The numerical model relies on state-of-the-art numerical methods for rapid computation of convolution products in the frequency domain, assisted by the very efficient fast Fourier transform algorithm for the discrete Fourier transform calculation. The displacement and stresses induced in tri-layered materials by arbitrary surface loads are computed based on analytical solutions existing in the frequency domain in the form of frequency response functions. A special conversion procedure is employed in this paper to obtain from these functions, the influence coefficients needed in the calculation of convolutions via the circular convolution theorem.

The developed computer program is checked for consistency with the one for bi-layered materials. A set of simulations is subsequently performed, showing the distribution of stresses in the layered systems under a contact load specific to a full-sliding regime. The site of the maximum equivalent stress, which is responsible for initiation of plastic yield or crack nucleation, is obtained. The presented simulations prove the method ability to support the design and testing of layered systems that provide increased performance and reliability under contact load.

6. ACKNOWLEDGEMENT

This work was partially supported from the project "Integrated Center for Research, Development and Innovation in Advanced Materials, Nanotechnologies, and Distributed Systems for Fabrication and Control", Contract No. 671/09.04.2015, Sectoral Operational Program for Increase of the Economic Competitiveness co-funded from the European Regional Development Fund.

7. REFERENCES

1. Chai H and Lawn B R 2004 *J. Mater. Res.* **19** 1752–1761;
2. Chai H and Lawn B R 2002 *Acta Mater.* **50** 2613–2625;
3. Katta R R, Nunez E E, Polycarpou A A, and Lee S-C 2009 *Microsyst. Technol.* **15** 1097–1110;
4. Kot M, Rakowski W, Lackner J M, and Major L 2013 *Mater. Des.* **43** 99–111;
5. Gorishnyy T Z, Olson L G, Oden M, Aouadi S M, and Rohde S L 2003 *J. Vac. Sci. Technol. A* **21** 332–339;
6. Chen J and Bull S J 2009 *Thin Solid Films* **517** 3704–3711;
7. Djabella H and Arnell R D 1994 *Thin Solid Films* **245** 27–33;
8. Komvopoulos K 1988 *J. Tribol. – Trans. ASME* **110** 477–485;
9. Luo J F, Liu Y J, and Berger E J 2000 *Comput. Mech.* **24** 448–455;
10. Chen W W, Zhou K, Keer L M, and Wang Q J 2010 *Int. J. Solids Struct.* **47** 2841–2854;
11. Zhou K, Keer L M, and Wang, Q J 2011 *J. Mech. Mater. Struct.* **6** 627–639;

12. Bagault C, Nelias D, Baietto M C, and Ovaert T C 2013 *Int. J. Solids Struct.* **50** 743–754;
13. O'Sullivian T C and King R B 1988 *J. Tribol. – Trans. ASME* **110** 235–240;
14. Nogi T and Kato T 1997 *J. Tribol. – Trans. ASME* **119** 493–500;
15. Liu S B and Wang Q 2002 *J. Tribol. – Trans. ASME* **124** 36–45;
16. Cai S and Bhushan B 2005 Wear **259** 1408–1423
17. Yu C, Wang Z, and Wang Q J 2014 *Mech. Mater.* **76** 102–120;
18. Wang Z, Yu C, and Wang Q J 2015 *Int. J. Solids Struct.* **66** 46–61;
19. Wang Z, Yu C, and Wang Q 2015 *J. Tribol. – Trans. ASME* **137** 011501;
20. Yu C, Wang Z, Liu G, Keer L M, Wang Q J 2016 *J. Tribol. – Trans. ASME* **138** 041402;
21. Spinu S 2019 *Tribology in Industry* **41** 242-253;
22. Spinu S 2020 *Tribology in Industry* **42** 131-145;
23. Liu S B, Wang Q and Liu G 2000 *Wear* **243** 101–111;
24. Polonsky I A and Keer L M 1999 *Wear* **231** 206–219;
25. Kalker J J and Van Randen Y 1972 *J Eng Math* **6** 193–206;
26. Wang Q J, Sun L, Zhang X, Liu S, and Zhu D 2020 *Front. Mech. Eng.* **6** 61.

Received: March 06, 2021 / Accepted: December 20, 2021 / Paper available online: December 25, 2021 © International Journal of Modern Manufacturing Technologies